Inorg. Chem. **2006**, *45*, 9643–9645

Redox-Controlled Molecular Flipper Based on a Chiral Cu Complex

Anna Company,[†] Mireia GUell,[†] Dana Popa,[†] Jordi Benet-Buchholz,[‡] Teodor Parella,[§] Xavier Fontrodona,[†] Antoni Llobet,[‡,§] Miquel Solà,[†] Xavi Ribas,[†] Josep M. Luis,*[,†] and Miquel Costas*[,†]

Departament de Química and Institut de Química Computacional, Universitat de Girona, Campus de Montilivi, E-17071 Girona, Spain, Institute of Chemical Research of Catalonia, Avinguda Països Catalans 16, Campus Universitari, E-43007 Tarragona, Spain, and Servei de RMN and Departament de Química, Universitat Autònoma de Barcelona, Bellaterra, E-08193 Barcelona, Spain

Received September 27, 2006

A molecular bipaddled flipper based on a tetradentate chiral Cu complex has been designed. The paddling motion of this unprecedented molecular-scale machine can be controlled by reversible oxidation of the metal center. Kinetic and computational (density functional theory) analyses provide a detailed picture of the flipper motion at the molecular scale, rationalize the switching role of the metal-ion oxidation state, and pose the basis for the fine-tuning of the dynamic motion of this new class of molecular-scale devices.

Molecular machines can transfer energy, motion, or forces at molecular scale, and their design constitutes a major goal in modern science and technology.[1] The design of these engines relies on the use of molecules that can undergo well-defined changes in shape in response to an external stimulus such as thermal, electrochemical, or photochemical excitation. Along this path, molecular rotors, gears, switches, shuttles, turnstiles, ratchets, brakes, and pedals have been designed over the last years and constitute the necessary basis for building more sophisticated multimolecular devices.[1−3] Because of basic thermodynamic considerations, molecular machines could only work under thermodynamic nonequilibrium conditions, a requisite not fulfilled by many of the earlier described molecular-scale devices. However, these molecules provide a useful nanotool kit to engineer complex machines built from organized gearing of different devices, capable of transferring the motion as a unit under the influence of an external equilibrium-breaking stimulus.[1−3] Inspired by the work of Canary on Cu-based molecular switches[4] and the well-established dynamic properties of copper(I) polyamine complexes,[5] in this work we describe an unprecedented molecular flipper whose motion is based on the isomerization process of a transition-metal complex. This motion is established at the molecular scale by a combination of kinetic and computational methods. It is also shown that the flipper can be switched on/off by reversible oxidation of the metal center, which can be viewed as an electrochemical brake.[6]

To this end, Δ-[Cu^{I}((N_R,N_R,R,R)-L)]PF_6 (**Δ-1PF$_6$**) was isolated as the single product from the reaction of ((1*R*,2*R*)-L) and $Cu^{I}(CH_3CN)_4PF_6$ in CH_3CN (Supporting Information) and structurally characterized. The molecular structure of **Δ-1PF$_6$**[7] (Scheme 1 and Figure 1) contains a Cu^{I} ion coordinated to the four N atoms of the ligand adopting a highly distorted tetrahedral geometry and a noncoordinating PF_6^- counterion balancing the charge. The complex contains a crystallographic 2-fold axis that passes through the Cu atom and bisects the cyclohexyl ring. This 2-fold symmetry results

* To whom correspondence should be addressed. E-mail: miquel.costas@udg.es (M.C.); josepm@iqc.udg.es (J.M.L.).
† Universitat de Girona.
‡ Institute of Chemical Research of Catalonia.
§ Universitat Autònoma de Barcelona.

(1) (a) Balzani, V.; Credi, A.; Raymo, F. M.; Stoddart, J. F. *Angew. Chem., Int. Ed.* **2000**, *39*, 3348. (b) *Struct. Bonding (Berlin)* **2001**, 99. Issue on Molecular Machines and Motors. (c) Balzani, V.; Venturi, M.; Credi, A. *Molecular Devices and Machines: A Journey into the Nanoworld*; Wiley-VCH: Weinheim, Germany, 2003. (d) Balzani, V.; Credi, A.; Venturi, M. *Molecular Devices and Machines*; Wiley-VCH: Weinheim, Germany, 2003. (e) Balzani, V.; Ceroni, P.; Ferrer, B. *Pure Appl. Chem.* **2004**, *76*, 1887.

(2) (a) Kinbara, K.; Aida, T. *Chem. Rev.* **2005**, *105*, 1377. (b) Kottas, G. S.; Clarke, L. I.; Horinek, D.; Michl, J. *Chem. Rev.* **2005**, *105*, 1281. (c) ter Wiel, M. K. J.; van Delden, R. A.; Meetsma, A.; Feringa, B. L. *J. Am. Chem. Soc.* **2005**, *127*, 14208. (d) Feringa, B. L.; van Delden, R. A.; ter Wiel, M. K. J. *Pure Appl. Chem.* **2003**, *75*, 563. (e) Chatterjee, M. N.; Kay, E. R.; Leigh D. A. *J. Am. Chem. Soc.* **2006**, *128*, 4058. (f) Hernández, J. V.; Kay, E. R.; Leigh, D. A. *Science* **2004**, *306*, 1532. (g) Khuong, T.-A. V.; Nunez, J. E.; Godinez, C. E.; Garcia-Garibay, M. A. *Acc. Chem. Res.* **2006**, *39*, 413. (h) Fonseca Guerra, C.; van der Wijst, T.; Bickelhaupt, F. M. *Chem.—Eur. J.* **2006**, *12*, 3032.

(3) (a) Muraoka, T.; Kinbara, K.; Aida, T. *Nature* **2006**, *440*, 512. (b) Badjic, J. D.; Balzani, V.; Credi, A.; Silvi, S.; Stoddart, J. F. *Science* **2004**, *303*, 1845. (c) Balzani, V.; Clemente-León, M.; Credi, A.; Ferrer, B.; Venturi, M.; Flood, A. H.; Stoddart, F. J. *Proc. Natl. Acad. Sci. U.S.A.* **2006**, *103*, 11.

(4) (a) Zahn, S.; Canary, J. W. *Science* **2000**, *288*, 1404. (b) Zahn, S.; Canary, J. W. *J. Am. Chem. Soc.* **2002**, *124*, 9204. (c) Zhang, J.; Siu, K.; Lin, C. H.; Canary, J. W. *New J. Chem.* **2005**, *29*, 1147.

(5) (a) Van Stein, G. C.; Van Koten, G.; de Bok, B.; Taylor, L. C.; Vrieze, K.; Brevard, C. *Inorg. Chim. Acta* **1984**, *89*, 29. (b) Riesgo, E.; Hu, Y.-Z.; Bouvier, F.; Thummel, R. P. *Inorg. Chem.* **2001**, *40*, 2541. (c) Pianet, I.; Vincent, J.-M. *Inorg. Chem.* **2004**, *43*, 2947. (d) Schultz, D.; Nitschke, J. R. *J. Am. Chem. Soc.* **2006**, *128*, 9887.

(6) Jog, P. V.; Brown, R. E.; Bates, D. K. *J. Org. Chem.* **2003**, *68*, 8240. (b) Kelly, T. R.; Bowyer, M. C.; Bhaskar, K. V.; Bebbington, D.; Garcia, A.; Lang, F.; Kim, M. H.; Jette, M. P. *J. Am. Chem. Soc.* **1994**, *116*, 3657.

10.1021/ic0618549 CCC: $33.50
Published on Web 11/04/2006

Scheme 1

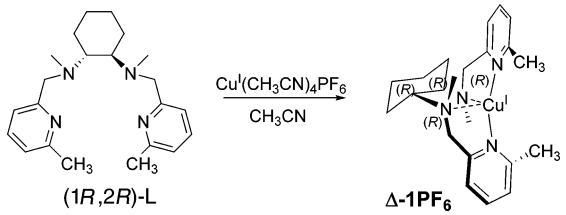

in a propeller-like structure in which the orientation of the rotation axis is determined by the chirality of the four stereogenic centers, adopting a Δ helicate chirality for the N_R,N_R,R,R isomer (Figure 1).

Time-dependent NMR analysis of **Δ-1PF$_6$** in CD_2Cl_2 indicates that the complex undergoes a transformation into a new 2-fold symmetric species **Λ-2PF$_6$**. A final K_{eq} = [**Λ-2PF$_6$**]/[**Δ-1PF$_6$**] = 1.3 at 298 K was measured at the end of the reaction ($\Delta G^o = -0.2$ kcal mol^{-1}), indicating a slight energetic preference for **Λ-2PF$_6$** in solution. K_{eq} = 1.3 persists in the temperature range from 10 to 35 °C, but crystallization by ether diffusion leads to quantitative recovery of **Δ-1PF$_6$**.[8] The structure of **Λ-2PF$_6$** was established as Λ-[Cu^I((N$_S$,N$_S$,R,R)-L)]PF$_6$ by NMR spectroscopy and density functional theory (DFT) calculations (Supporting Information). **Δ-1PF$_6$** and **Λ-2PF$_6$** are related by inversion of the chirality of the aliphatic N atoms but most significantly by the opposite helicate chirality.

The circular dichroism (CD) spectrum of a freshly prepared solution of **Δ-1PF$_6$** in CH_2Cl_2 displays negative curves with large amplitudes at 268 nm ($\Delta\epsilon = -11.5$ M^{-1} cm^{-1}) and 350 nm ($\Delta\epsilon = -4.4$ M^{-1} cm^{-1}) and a prominent positive curve at 290 nm ($\Delta\epsilon = 8.7$ M^{-1} cm^{-1}). The **Δ-1PF$_6$** to **Λ-2PF$_6$** isomerization reaction was monitored by CD (Figure 2), showing a quenching of the differential absorption at 268, 290, and 350 nm. Kinetic traces of the CD data were fitted to a reversible single-exponential process, where the two reversal reactions (k_1 and k_{-1}) are unimolecular. Isomerization rate constants in CH_2Cl_2 at 298 K are $k_1 = 2.8\ (\pm 0.1) \times 10^{-4}$ s^{-1} and $k_{-1} = 2.1\ (\pm 0.1) \times 10^{-4}$ s^{-1}, and they are

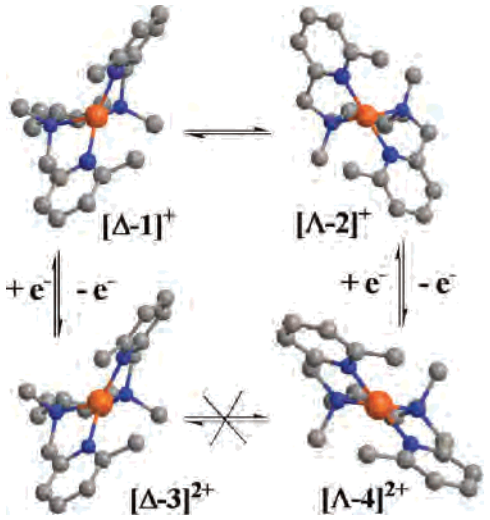

Figure 1. Crystal structure (Mercury diagram) of [**Δ-1**]$^+$ (top left) and DFT structures of [**Λ-2**]$^+$ (top right), [**Δ-3**]$^{2+}$ (bottom left), and [**Λ-4**]$^{2+}$ (bottom right).

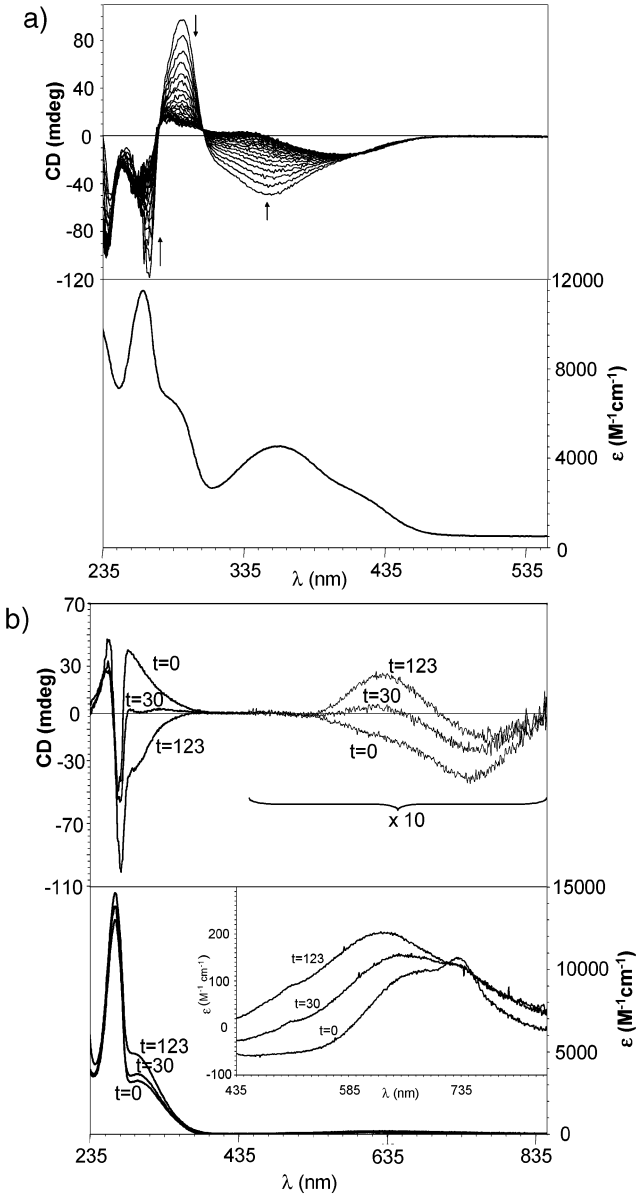

Figure 2. (a) Top: CD monitoring of the **Δ-1PF$_6$**/**Λ-2PF$_6$** isomerization reaction in CH_2Cl_2 ([**1**]$_0$ = 0.34 mM, path length = 1 cm, spectrum interval = 5 min). Bottom: corresponding UV−vis spectra. (b) Top: CD spectra of the oxidized **Δ-1PF$_6$**/**Λ-2PF$_6$** couple with $AgBF_4$ at different isomerization times (min) yielding [**Δ-3**]$^{2+}$ at $t = 0$ min and mixtures of [**Δ-3**]$^{2+}$ and [**Λ-4**]$^{2+}$ at $t > 0$ min. Bottom: corresponding UV−vis spectra.

concentration-independent in the 0.1−1 mM range, thus confirming their unimolecular nature. Eyring plots for k_1 and

(7) Crystal data for **Δ-1PF$_6$**: Bruker CCD diffractometer, $C_{22}H_{32}CuF_6N_4P$, fw = 561.03, 0.4 × 0.1 × 0.05 mm, orthorhombic, space group $P2_12_12$, a = 16.921(3) Å, b = 34.176(6) Å, c = 8.4534(15) Å, α = 90°, β = 90°, γ = 90°, V = 4888.4(15) Å^3, D_c = 1.525 g cm^{-3}, Z = 4, monochromated Mo Kα radiation, φ and ω scan methods, T = 100(2) K, μ = 1.023 mm^{-1}, 76 923 reflections collected, 11 939 independent reflections (R_{int} = 0.0480), GOF = 1.065, R [$I > 2\sigma(I)$] = 0.0415, wR = 0.1013 (refined against $|F^2|$).

(8) A number of attempts have been made to obtain crystallographic characterization of **Λ-2X** (X = CF_3SO_3, PF_6, BF_4, SbF_6, and ClO_4), but in all cases, **Δ-1X** is the single product isolated.

(9) Zn reduction is slow and affords isomeric **Δ-1PF$_6$**/**Λ-2PF$_6$** mixtures. Ag^I oxidation results in Ag precipitation, and no Zn^{II} complexes were formed upon reaction with metallic Zn, as ascertained by NMR spectroscopy.

(10) (a) Becke, A. D. *J. Chem. Phys.* **1993**, *98*, 5648. (b) Lee, C.; Yang, W.; Parr, R. G. *Phys. Rev. B* **1988**, *37*, 785.

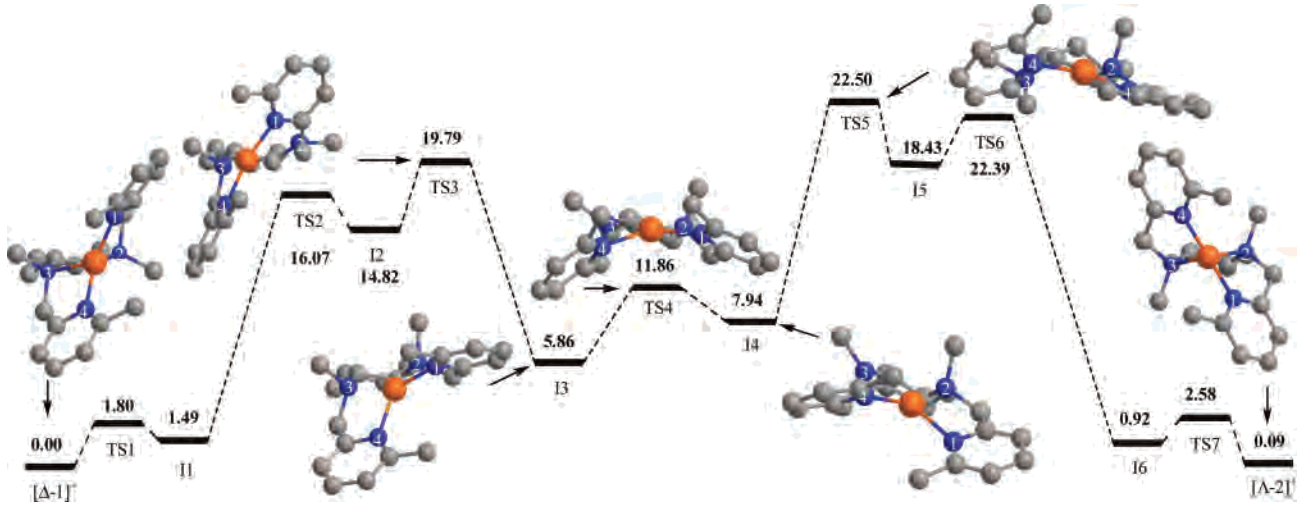

Figure 3. Calculated reaction pathway of the $[\mathbf{\Delta\text{-}1}]^+ \rightarrow [\mathbf{\Lambda\text{-}2}]^+$ isomerization with B3LYP/6-311G(d,p) Gibbs free energies at 298.15 K (kcal mol^{-1}).

k_{-1} in the 10−35 °C temperature range provide enthalpy and entropy activation parameters (Table S1 in the Supporting Information). Thermal excitation has a profound effect on the isomerization rate, indicating that the enthalpic contribution accounts for the most important part of the activation barrier.

The mechanical motion undergone by **Δ-1PF$_6$** and **Λ-2PF$_6$** could be switched on/off by reversible metal oxidation. Cyclic voltammetry in CH_2Cl_2 indicates that **Δ-1PF$_6$** and **Λ-2PF$_6$** could be electrochemically oxidized ($E_{1/2} = 0.59$ V vs SSCE, $I_{ap}/I_{cp} \sim 1$) to the corresponding Cu^{II} complexes. Alternatively, **Δ-1PF$_6$** and **Λ-2PF$_6$** can be reversibly oxidized and reduced chemically with Ag^+ and Zn,[9] respectively. An oxidation experiment of species **Δ-1PF$_6$** with $AgBF_4$ was performed at different times of the isomerization process and the CD of the resulting Cu^{II} species registered (Figure 2). The registered spectra progressively change depending on the degree of $[\mathbf{\Delta\text{-}1}]^+/[\mathbf{\Lambda\text{-}2}]^+$ isomerization. However, no further changes were observed after oxidation over more than 1 week, thus indicating that the paddling motion has been stopped.

To give a detailed molecular picture of the isomerization process, the system was studied by means of DFT. The gas-phase geometries, energies, and vibrational frequencies of $[\mathbf{\Delta\text{-}1}]^+$, $[\mathbf{\Lambda\text{-}2}]^+$, and several intermediates and transition states labeled in Figure 3 were computed using the B3LYP[10] functional. We use the 6-31G(d,p) basis set to determine the geometries and vibrational frequencies, whereas the energies were obtained by carrying out single-point 6-311G(d,p) calculations at the 6-31G(d,p) geometries. The $[\mathbf{\Delta\text{-}1}]^+/[\mathbf{\Lambda\text{-}2}]^+$ isomerization has a complex mechanism with six intermediates and seven transition states (see the Supporting Information for details). There is a good agreement between the experimental crystal structure of **Δ-1PF$_6$** and the corresponding B3LYP geometry of $[\mathbf{\Delta\text{-}1}]^+$. The steps of the isomerization mechanism can be split into three main stages. The first stage ends in I3 and involves the rotation of the N^2CH_3 group from a $CH_3N^2-N^3CH_3$ trans-like orientation to a cis-like orientation. This rotation also implies the transformation of one N_R to N_S. The second stage finishes at I4, and the most important feature is the paddling movement of the two pyridylmethyl groups. Finally the last stage involves the rotation of the other N^3CH_3 group and the transformation of the second N_R to N_S. TS3 and TS4 give the limiting steps of the first and second stages, respectively. However, the limiting step of the $[\mathbf{\Delta\text{-}1}]^+/[\mathbf{\Lambda\text{-}2}]^+$ isomerization is given by TS5 of the third stage, which has a free energy of 22.50 kcal mol^{-1} above $[\mathbf{\Delta\text{-}1}]^+$. The computationally determined free energy barrier is in good agreement with the experimental data of $\Delta G_1^{\ddagger\circ}$ and $\Delta G_{-1}^{\ddagger\circ}$ presented in Table S1 in the Supporting Information. DFT analysis also provides an explanation for the role of the oxidation state of the metal in controlling the motion. The theoretically computed $[\mathbf{\Delta\text{-}3}]^{2+}/[\mathbf{\Lambda\text{-}4}]^{2+}$ isomerization has the same three stages as the $[\mathbf{\Delta\text{-}1}]^+/[\mathbf{\Lambda\text{-}2}]^+$ isomerization, and also the limiting step is given by TS5′, which is 36.19 and 37.60 kcal mol^{-1} higher than $[\mathbf{\Delta\text{-}3}]^{2+}$ and $[\mathbf{\Lambda\text{-}4}]^{2+}$, respectively. It is clear that $\Delta G_1^{\ddagger\circ}$ and $\Delta G_{-1}^{\ddagger\circ}$ for these processes are prohibitively high for a normal solution-phase thermal reaction (Figure 1).

In conclusion, in this work we have described at the molecular scale the mechanical motion exhibited by $[\mathbf{\Delta\text{-}1}]^+/[\mathbf{\Lambda\text{-}2}]^+$ isomerization. The transition metal integrated into this device acts as a redox switch that permits one to start/stop the motion at will. The well-defined molecular paddling motion as well as its redox control adds to the currently available nanotool box, makes these molecules suitable components for yet-to-build molecular machines, and could be particularly useful in acting as a brake of the machine.

Acknowledgment. This research has been financed by MCYT Project BQU2003-02884, MEC Project CTQ2005-08797-C02-01/BQU, and MEC Project CSD2006-0003. A.C. and M.G. are thankful for a predoctoral grant from MEC. X.R. is thankful for a JdC contract from MEC.

Supporting Information Available: Full details of the synthetic procedures, spectroscopic characterization of products, kinetic analysis, DFT-optimized coordinates of all minima and transition states located, and X-ray crystallographic data (CIF). This material is available free of charge via the Internet at http://pubs.acs.org.

IC0618549